Size effect predictions by fracture models for a refractory ceramic

International Journal of Fracture **75**: 273–283, 1996.

Size effect predictions by fracture models for a refractory ceramic

M.A.J. VAN GILS, L.J.M.G. DORTMANS and G. DE WITH
Centre for Technical Ceramics, P.O.Box 595, 5600 AN Eindhoven, The Netherlands

W.A.M. BREKELMANS and J.H.P. DE VREE
Eindhoven University of Technology, Faculty of Mechanical Engineering, P.O.Box 513, 5600 MB Eindhoven, The Netherlands

Received January 1995; accepted in revised form 24 October 1995

Abstract. Refractory ceramics used as kiln furniture are designed to operate at elevated temperatures with a high thermal shock resistance. In practice, however, the material fails due to thermal fatigue after a limited number of cycles. To predict this failure behaviour, it is generally not possible to use linear elastic fracture mechanics due to the fact that the coarse grained, porous material shows a dissipative mechanical behaviour. Differently sized specimens are tested to determine the size effect associated with this material. Four different finite element models widely used for concrete modelling are investigated on their ability to describe this nonlinear failure behaviour, in particular the associated size effect phenomenon. The results of the initially promising Nonlocal Continuum Damage Mechanics (CDM) model indicate that this approach cannot properly describe the observed size effect. The other three models (Adapted Local CDM, Fictitious Crack and Smeared Crack), however, give comparable results with a good description of the observed size effect phenomenon.

1. Introduction

When designing structures, knowledge of the failure behaviour of the materials used is of major importance in order to obtain a safe design with a satisfying life time. The ultimate aim of the present research is to model crack initiation and propagation within a ceramic component, a so-called plate saggar. This component is made of a refractory ceramic, tradename Alcorit (Sphinx Technical Ceramics), and is used as support for a plate during firing. The plate saggars fail after a number of temperature cycles between room temperature and 1200 °C due to thermal stresses.

In order to achieve a useful numerical model which describes the fracture process in the plate saggar, it is necessary to obtain insight into the crack growth process under controlled circumstances. To accomplish this, the description of the material behaviour at room temperature subjected to mode I loading is taken as the point of departure. In a later stage the effect of different loadings, temperature changes and other geometries will be taken into account.

The classical method to describe crack growth processes applies the theory of Linear Elastic Fracture Mechanics (LEFM). The disadvantage of this theory is the difficulty of incorporating the LEFM criteria in the Finite Element (FE) method. Nevertheless, the LEFM theory is still an often used and also valid model for describing crack propagation in (purely) brittle materials. LEFM models can therefore serve as a reference to compare with other models. All models should converge to the LEFM results for an infinite size of the structure. Deviations from the LEFM theory occur only for finite dimensions as is found from experimental data discussed in Section 4.

For the explanation of these deviations from LEFM theory, research done in the field of concrete cracking can give an indication in the proper direction. From observations of the crack tip in concrete and in ceramics, it appears that nonlinear phenomena occur in front of the crack tip, in the so-called process zone. To describe the crack growth in a material containing cracks with a process zone, several FE models have been developed. Four important models are the Fictitious Crack (FC) model [9, 11, 14], the Smeared Crack (SC) model [13, 14], the Nonlocal Continuum Damage Mechanics (NLCDM) model [10, 12, 17] and the Adapted Local Continuum Damage Mechanics (ALCDM) model [4, 5]. The major difference between these models is the way in which strain localization is described. With respect to this strain localization it seems plausible that strains are localized in a gradually distributed way. Difficulties in implementing this general hypothesis have lead to more simple criteria, such as localization within a band or along a line. Among the previously mentioned FE models, the NLCDM model results in a smooth strain localization, the SC model and the ALCDM in a localization within a band and the FC model in a crack line localization.

In order to discriminate between the models mentioned above, an important phenomenon resulting from fracture mechanics, the so-called size effect, will be considered. This size effect can be defined as the dependence of the maximum sustainable nominal stress of a structure (maximum load divided by a relevant surface measure of the structure) on the size of this structure. To separate the size effect from other influences, structures with geometrically similar shapes (e.g., beams with the same span-to-depth ratio and the same crack length-to-depth ratio) should be examined. Due to nonlinear material behaviour a deviation from the size effect as predicted by LEFM will occur. For smaller structures these deviations will become more pronounced because the size of the process zone is assumed to be determined by the material properties. For structures with a size large enough compared to the size of the process zone, the influence of this process zone will be negligible and LEFM theory will be applicable.

In this paper the size effect associated with Alcorit is investigated using differently sized specimens. The four FE models will be investigated on their ability to describe this size effect. A simple configuration, the single edge notched beam, often used in both experimental and numerical analyses, will be evaluated. Attention will be focused on the maximum loads c.q. the load bearing capacity, because this property is believed to be the most important feature. In a later stage the softening curve will be investigated in order to complete the model. The maximum loads as predicted by the different models will provide the input for the Bažant Size Effect Law which will be discussed in Section 3. In this way material properties like fracture energy and process zone size can be calculated and compared with the values which were originally used as input in the FE models.

The approach suggested above will give information on the relation of the Bažant Size Effect Law and the FE models as well as information on the comparison of the FE models mutually. It must be emphasized that the analyses are focused on mode I loading and that therefore conclusions cannot be simply generalized to other loading conditions.

2. Experiments

In order to evaluate the mechanical behaviour of the refractory ceramic two types of mode I experiments have been set up. These experiments use the well-known Single Edge Notched Beam (SENB) and the so-called Wedge Opening Loaded (WOL) configuration [6, 15], respectively. The two configurations are shown in Figure 1 and Figure 2. With these two geometries a large range in specimen size can be tested in order to establish the size effect. The specimen sizes used, are listed in Table 1.

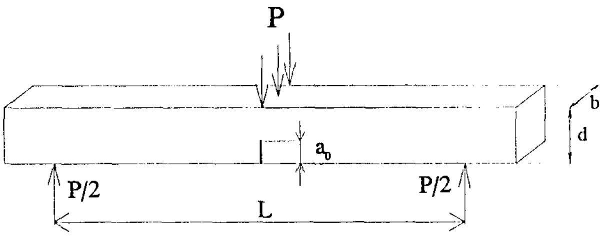

Figure 1. SENB configuration.

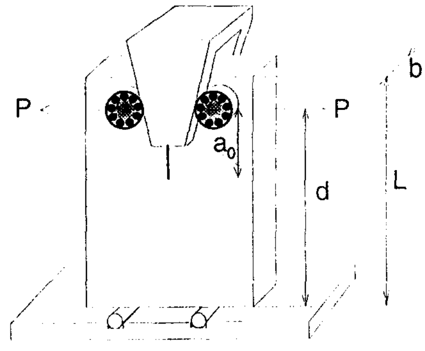

Figure 2. WOL configuration.

Table 1. Specimen sizes for SENB and WOL geometry

	d [mm]	b [mm]	L [mm]	$\alpha_0 = a_0/d$ [-]
SENB	10-50	10-50	4d	0.25, 0.75
WOL	120	30	151	0.25, 0.5

3. Size effect law according to Bažant

Based on observations of the size effect associated with concrete, Bažant has proposed the so-called Size Effect Law (SEL) to predict size- and shape-independent material properties like the true fracture energy and the size of the fracture process zone [1, 3]. For materials that do not behave according to the LEFM theory it is not evident how to determine these material properties because the use of specimens of different size will result in different values for the fracture energy. These values will not only depend on the size of the structure c.q. the size of the crack, but also on the shape of the structure. Bažant states that for each material there exist two size- and shape-independent material properties. These two material properties are the fracture energy G_f and the equivalent size of the process zone c_f, occurring for infinitely large specimens. With these two parameters Bažant's Size Effect Law becomes

$$\tau_{\text{nom}} = \sqrt{\frac{E'G_f}{c_f + \bar{d}}}, \tag{1}$$

where the nominal strength τ_{nom} and effective size $\bar{d}$ for two-dimensional structures are defined by

$$\tau_{\text{nom}} = \frac{P_{\text{max}}}{A}\sqrt{g'(\alpha_0)}, \tag{2}$$

$$\bar{d} = \frac{g(\alpha_0)}{g'(\alpha_0)}d, \tag{3}$$

with

$$E' = \left\{ \begin{array}{ll} E & \text{in case of plane stress} \\ \dfrac{E}{1-\nu^2} & \text{in case of plane strain} \end{array} \right\},$$

E = Young's modulus,

ν = Poisson's ratio,

$P_{\max}$ = maximum sustainable force,

A = characteristic surface measure,

α_0 = a_0/d = relative crack length,

$g(\alpha)$ = non-dimensional function depending on α and resulting from LEFM analysis,

$g'(\alpha) = \dfrac{\mathrm{d}g(\alpha)}{\mathrm{d}\alpha}$.

For a single edge notched beam with $L/d = 4$, the function $g(\alpha)$ is defined by Srawley [16]:

$$g(\alpha) = 36\frac{\alpha\left(1.99 - \alpha(1-\alpha)(2.15 - 3.93\alpha + 2.7\alpha^2)\right)^2}{(1+2\alpha)^2(1-\alpha)^3}, \tag{4}$$

and for the WOL geometry by Saxena and Hudak [15]:

$$g(\alpha) = \frac{(2+\alpha)^2(0.8072 + 8.858\alpha - 30.23\alpha^2 + 41.088\alpha^3 - 24.14\alpha^4 + 4.951\alpha^5)^2}{(1-\alpha)^3}. \tag{5}$$

For both geometries the surface measure A is defined by $A = b \cdot d$.

4. Experimental results

With the maximum loads obtained from the test specimens as described in Section 2, the size effect associated with Alcorit can be investigated using Bažant's SEL. For each specimen tested, the values of the effective size $\bar{d}$ and nominal stress τ_N are calculated. The parameters of Bažant's SEL are estimated using the method of least squares. The resulting size effect graph with the experimental results and the fit according to Bažant's SEL is illustrated in Figure 3. From Figure 3 it may be concluded that the trend of the observed size effect of Alcorit is similar to that of Bažant's SEL. The material shows a strong size effect with the strongest deviation from the LEFM theory occurring for the smallest SENB specimens.

5. FE models

As demonstrated in the previous section Bažant's SEL gives a good description of the observed size effect of Alcorit. Therefore the Bažant SEL will be used to compare four different FE models with respect to their ability to predict this size effect. These models are the Fictitious Crack (FC) model, the multi-directional Smeared Crack (SC) model, the Nonlocal Continuum Damage Mechanics (NLCDM) model and an Adapted Local Continuum Damage Mechanics (ALCDM) model. In this section a short introduction in the fundamentals of these models will be presented.

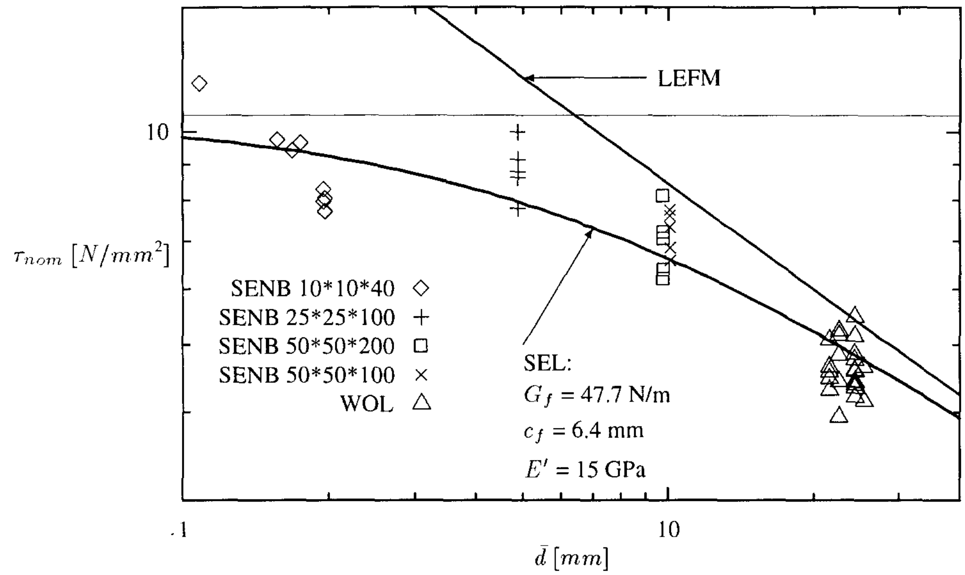

Figure 3. Experimental results.

5.1. FICTITIOUS CRACK MODEL

The Fictitious Crack model [9, 11, 14], also called the Discrete Crack model, is inspired by the classical Dugdale–Barenblatt crack concept. Interface elements are placed between the continuum elements to discretize the crack path. When the normal stress in a certain interface point exceeds the tensile strength f_t of the material, a softening constitutive behaviour is introduced in that interface point. The interface nodes connecting the continuum elements then separate, thus simulating the crack opening. The constitutive cracking behaviour is determined by the stress/crack-opening relationship, where the area under this stress/crack-opening curve equals the fracture energy G_f of the material.

5.2. SMEARED CRACK MODEL

In the multi-directional Smeared Crack model [13, 14], a crack is simulated by introducing a softening anisotropic constitutive behaviour in element integration points in which a certain stress limit is reached. The major difference with the Fictitious Crack model is the fact that the cracking behaviour is modelled in terms of stress/strain instead of stress/displacement relationships. As a result, the dissipated energy depends on the volume associated with integration points. In order to predict a correct energy dissipation, the size of the elements c.q. the volume associated with the integration points should correspond to a characteristic length parameter. This length parameter is called the crack band width and is usually taken equal to three times the maximum grain size.

5.3. NONLOCAL CONTINUUM DAMAGE MECHANICS MODEL

The Nonlocal Continuum Damage Mechanics model [10, 12, 17] introduces an internal variable in the constitutive equations. This internal damage variable induces a softening material behaviour when a strain measure (to be defined) exceeds a certain threshold. The present model uses an isotropic damage parameter D influencing the constitutive behaviour in a way introduced by Kachanov and adopted by numerous researchers [2, 10]:

$$\sigma = (1 - D)\mathbf{C} : \varepsilon, \tag{6}$$

where σ is the stress tensor; $\mathbf{C}$ is the elasticity tensor; and ε is the strain tensor.

The evolution of the damage parameter is coupled to the development of strains. At local level a modified von Mises equivalent strain [17] is used

$$\varepsilon_{\mathrm{eq}} = \frac{k-1}{2k(1-2\nu)}J_1 + \frac{1}{2k}\sqrt{\left(\frac{k-1}{1-2\nu}J_1\right)^2 - \frac{12k}{(1+\nu)^2}J_2'}, \tag{7}$$

with the strain invariants:

$$J_1 = \mathrm{tr}(\boldsymbol{\varepsilon}), \tag{8}$$

$$J_2' = -\tfrac{1}{6}\left\{3\mathrm{tr}(\boldsymbol{\varepsilon}\cdot\boldsymbol{\varepsilon}) - (\mathrm{tr}(\boldsymbol{\varepsilon}))^2\right\}, \tag{9}$$

and with k the ratio of the compressive strength f_c and the tensile strength f_t

$$k = \frac{f_c}{f_t}. \tag{10}$$

To avoid mesh-sensitivity, strain localization is regularized by the introduction of a nonlocal equivalent strain defined by

$$\bar{\varepsilon}_{\mathrm{eq}}(\mathbf{x}) = \frac{1}{\int_{|\mathbf{r}|<\lambda} w(|\mathbf{r}|)\,\mathrm{d}V}\int_{|\mathbf{r}|<\lambda} w(|\mathbf{r}|)\varepsilon_{\mathrm{eq}}(\mathbf{x}+\mathbf{r})\,\mathrm{d}V, \tag{11}$$

with the introduction of the nonlocal weighing parameter λ, also called the characteristic length, and a Gaussian weight function:

$$w(|\mathbf{r}|) = \mathrm{e}^{-\left(\frac{2|\mathbf{r}|}{\lambda}\right)^2}. \tag{12}$$

The local actual damage is a function of the maximum value of the nonlocal equivalent strain $\bar{\varepsilon}_{\mathrm{eq}}$ above a particular threshold [10]. This function determines the character of the softening as a result of (6).

This framework of continuum damage modelling is different from the recent work of Elices et al. [8] and de Borst et al. [4] who split the strain tensor in an elastic and an inelastic part. The evolution of the damage parameter D in these papers is coupled to the evolution of the (nonlocal) *in*elastic strain. The major difference in comparison with the present work is that initiation of damage is based on a *non*local strain measure $\bar{\varepsilon}_{\mathrm{eq}}$ and in the work, [8] and [4], on a local stress measure (f_t).

5.4. ADAPTED LOCAL CONTINUUM DAMAGE MODEL

The Adapted Local CDM model [4, 5] is a refinement of the original CDM model in order to reduce the mesh-sensitivity. The present ALCDM model shows an adequate energy dissipation by adapting the material properties to the element size. The critical strain value ε_c, satisfying $D(\varepsilon_c) = 1$, will depend on a certain length L_e which is a representative value for the size of the element. For a linear softening constitutive relation this critical strain equals

$$\varepsilon_c = \frac{2 \cdot G_f}{f_t \cdot L_e}. \tag{13}$$

The characteristic size L_e for two-dimensional elements is defined by

$$L_e = \sqrt{A_E} \tag{14}$$

with A_E the area of the element. This definition of the characteristic length is of course only valid in the present situation where square elements were used in the FE mesh. The dependence of the dissipated energy on the element integration scheme is reduced by forcing the damage to be constant within an element.

6. Numerical results

To compare the models introduced in the previous section, the load-displacement curves of differently sized single edge notched beams are calculated. The beam sizes $(b \times d \times L)$ with $\alpha_0 = 0.25$, see Figure 1, are:

$$\begin{aligned}
2.5 &\times 2.5 \times 10\ \text{mm}^3 \ \text{(beam 1)},\\
10 &\times 10 \times 40\ \text{mm}^3 \ \text{(beam 2)},\\
25 &\times 25 \times 100\ \text{mm}^3 \ \text{(beam 3)},\\
50 &\times 50 \times 200\ \text{mm}^3 \ \text{(beam 4)}.
\end{aligned}$$

The material parameters are chosen so that they represent the refractory ceramic Alcorit most closely. The actual values of these material properties should be derived from the experiments, however, the experimental results were not available during the time of the calculations. The parameters used for the calculations are therefore reasonable estimations of the true values. For the softening curve, $\sigma(u)$ or $\sigma(\varepsilon)$, a constant slope (linear softening) is assumed with the following material parameters:

$$\begin{aligned}
f_t &= 9\ \text{MPa}, & G_f &= 30\ \text{N/m},\\
E &= 15\ \text{GPa}, & \lambda &= 2.5\ \text{mm},\\
\nu &= 0.25, & k &= 8.
\end{aligned}$$

Second order plane stress elements with four integration points were used in the analyses. The arc length method [7] was used for the largest beam to capture the snap-back behaviour in the force/displacement curve. Figures 4 and 5 display the force/associated displacement curves for the smallest and the largest beam using the different FE models.

These figures show that the larger beam behaves in a more brittle manner than the smaller beam as can be expected. For larger beams the deviation from the linear behaviour until

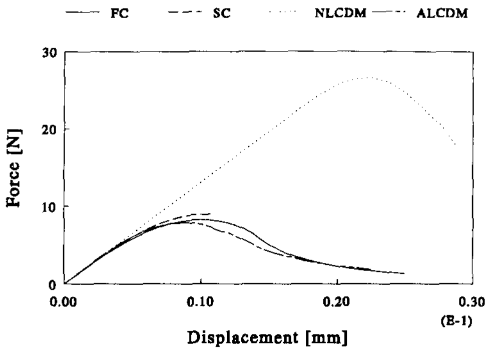

Figure 4. Force/displ. curves for beam 1.

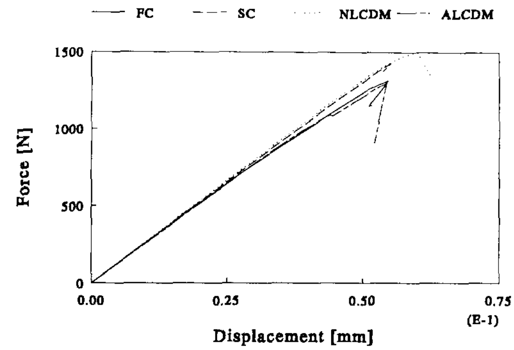

Figure 5. Force/displ. curves for beam 4.

Table 2. Size Effect Law parameters

FC	SC	NLCDM $\lambda = 2.5\,\mathrm{mm}$	ALCDM
$G_f = 26.1\,\mathrm{N/m}$	$G_f = 30.1\,\mathrm{N/m}$	$G_f = 31.2\,\mathrm{N/m}$	$G_f = 25.3\,\mathrm{N/m}$
$c_f = 1.05\,\mathrm{mm}$	$c_f = 1.03\,\mathrm{mm}$	$c_f = -0.31\,\mathrm{mm}$	$c_f = 1.13\,\mathrm{mm}$

maximum load decreases because the relative size of the process zone decreases. In Figure 4, a striking deviation of the NLCDM model from the other models can be observed. This deviation decreases for larger beams, see Figure 5. The other models result in almost identical curves with slight differences in the maximum loads. It can be concluded that the nonlocal formulation causes a strongly deviating prediction of the maximum loads and the dissipated energy when the nonlocal parameter λ becomes relatively large compared to the size of the structure. This effect can also be found in the size effect curves based on the maximum loads which are shown in Figures 6–9. For the NLCDM model several values of the characteristic length λ were evaluated (Figure 8). It appears that an increase of this characteristic length results in a steeper size effect curve. The parameters of Bažant's SEL fitted on the results of the different models are given in Table 2.

From the size effect curves it becomes clear that the present NLCDM model cannot describe the size effect as expected to occur in experiments. As a result of the weighing process the peak

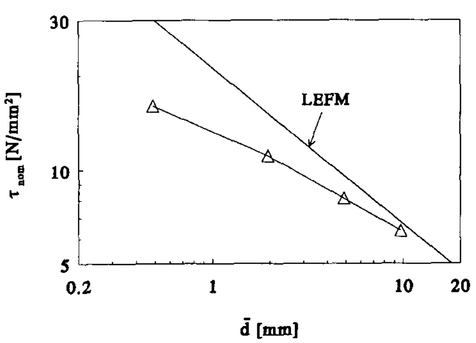

△ FC

Figure 6. Size effect FC model.

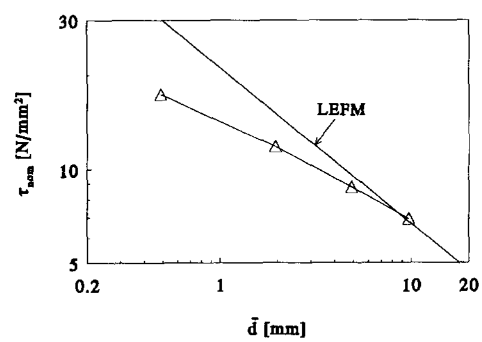

△ SC

Figure 7. Size effect SC model.

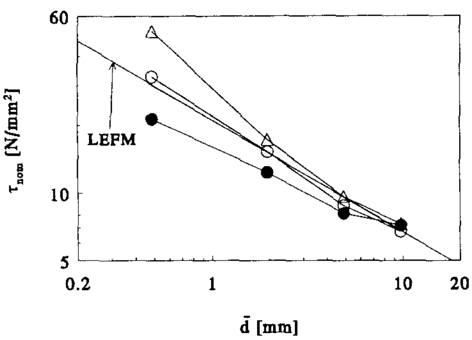

△ $\lambda = 2.5\,\text{mm}$ ○ $\lambda = 1.25\,\text{mm}$
• $\lambda = 0.625\,\text{mm}$

Figure 8. Size effect NLCDM model.

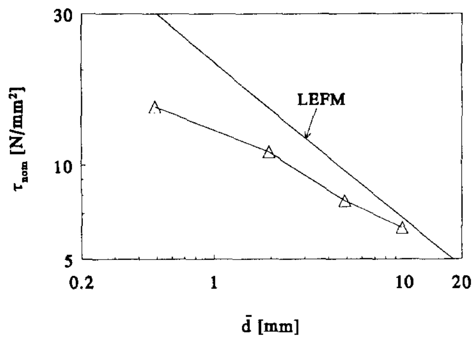

△ ALCDM

Figure 9. Size effect ALCDM model.

stresses at the crack tip decrease with increasing value of λ. This process has two remarkable effects:

- Increasing τ_{nom} with increasing λ. This is in contrast to the SEL where an increasing c_f results in a *decreasing* τ_{nom}. The effect of the nonlocal parameter λ and the effect of the effective process zone length c_f on the size effect are not comparable.
- The curvature $\frac{\partial^2 \ln \tau_{\text{nom}}}{\partial \ln^2 \bar{d}}$ is positive. This is true for all λ in a certain range of $\bar{d}$. According to the SEL, however, this curvature is always *negative* and according to LEFM it is equal to zero.

The three other models show comparable results with regard to the size effect and the fitted parameters G_f of Bažant' SEL show a relatively good agreement with the original value. The numerical values of the fracture energy G_f and the process zone length c_f are smaller than the experimental values obtained in Section 4. To obtain the experimental size effect curve the numerical input parameters G_f and f_t of the FE models should be adapted. A higher value for the fracture energy G_f ($G_f \approx 50$ N/m) and a lower value for the tensile strength f_t should be used in order to obtain the less brittle experimental response. It must be mentioned, however, that these models all show a slight deviation from the shape of the Bažant SEL (Figure 3).

7. Conclusions

From the experimental results it can be concluded that the refractory ceramic Alcorit shows a strong size effect which can be described with Bažant's SEL. A constitutive model describing nonlinear material behaviour should predict this size effect correctly.

The Fictitious Crack model has the disadvantage, especially in more complex geometries and loading conditions, that it is necessary to know *a priori* the crack path in order to model it with interface elements. Another disadvantage is the fact that the crack can only develop in mode I. Crack initiation due to shearing or high compressive loading is not possible. Nevertheless, the FC model can be considered as reference for other models and for determining (mode I) material parameters.

The Smeared Crack model suffers from mesh-dependence as a result of the absence of strain localizers in the model. The present method of manual adaptation of the input parameters can only be effective for those problems where the size of the crack band is known. For complicated geometries with different element sizes this method will not yield consistent data. Incorporating a sort of strain localization limiter or an automatic adaptation of the material parameters (as in the ALCDM model) could, however, result in an attractive model. The advantage of such a model is the fact that an anisotropic damage model based on stress/strain relations can simulate the actual cracking process without the need for complicated meshes containing interface elements

The Nonlocal CDM model gives results that converge with mesh-refinement and is probably the model that resembles the strain field in the localization zone most closely because it introduces a localization zone with gradually distributed strains. It suffers, however, from several problems due to the nonlocal formulation. The averaging process at the crack tip smears out the peak stresses, resulting in lower damage values and higher maximum loads. This causes a size effect which is incomparable with that of Bažant's SEL. Large values of the characteristic nonlocal length λ result in an increasing size effect in comparison with the LEFM model. It is possible that the deviation from the Bažant SEL will be less when the formulation of the nonlocal CDM model would be based on the use of a nonlocal inelastic strain and a local damage initiation threshold. The use of a local threshold causes, however, strain localization in case of a one-dimensional situation [8] which raises the question if mesh-independent result can still be guaranteed.

The Adapted Local CDM model doesn't have the nonlocal difficulties of the NLCDM model but can still give mesh-independent results with a proper description of the size effect. A disadvantage of this model, as well as for the SC model, is the fact that the size of the damage zone is mesh-dependent and not representative for the actual size of the localization zone. This fact doesn't, however, restrict the applicability of the model because the global response is hardly influenced.

The FC, SC and ALCDM models are principally all suitable to describe the experimentally observed size effect. An increasing deviation from the LEFM results can be seen for the nominal strength values in the case of smaller structures. The shape of the resulting size effect curve is somewhat different from the prediction of Bažant's SEL. Especially for smaller structures, the Bažant SEL nominal strength values are smaller than the FE results. Based on Bažant's SEL, preliminary estimations of the material properties can be determined. The correct shape of the size effect curve should follow from experiments.

An untouched issue is the fact that the present evaluation is restricted to mode I loading. The influence of mode II, mode III and mixed mode loading on the mechanical behaviour of the material and on the performance of the different damage models is unknown. Both experimental and numerical evaluations of test geometries displaying other stress fields will have to be carried out to completely evaluate the damage models for static loading at room temperature.

References

1. Z.P. Bažant, *Journal of Engineering Mechanics* 110(4) (1984) 518–535.
2. Z.P. Bažant and G. Pijaudier-Cabot, *Journal of Applied Mechanics* 55 (1988) 287–293.
3. Z.P. Bažant and M.T. Kazemi, *Journal of the American Ceramic Society* 73 (1990) 1841–1853.
4. R. de Borst and H.-B. Mühlhaus, in *Fracture Processes in Concrete, Rock and Ceramics* J.G.M. van Mier, J.G. Rots and A. Bakker (eds.), (1991) 601–618.
5. W.A.M. Brekelmans and J.H.P. de Vree, *Acta Mechanica* 110(1–4) (1995) 49–56.
6. E. Brühwiler and F.H. Wittmann, *Engineering Fracture Mechanics* 35(1/2/3) (1990) 117–125.
7. M.A. Crisfield, in *Numerical Methods for Non-linear Problems*, C. Taylor, E. Hinton and D.R.J. Owen (eds.), Pineridge Press, Swansea (1980) 261–290.

8. M. Elices, J. Planas and G.V. Guinea, in *Fracture and Damage of Concrete and Rock FDCR-2*, H.P. Rossmanith (ed.), (1993) 3–33.
9. A. Hillerborg, M. Modeer and P.E. Petersson, *Cement and Concrete Research* 6 (1976) 773–782.
10. C. Saouridis and J. Mazars, in *Cracking and Damage, Strain Localization and Size Effect*, J. Mazars and Z.P. Bažant (eds.), (1998) 391–403.
11. D. Ngo and A.C. Scordelis, *Journal of the American Concrete Institute* 64(14) (1967) 152–163.
12. G. Pijaudier-Cabot and Z.P. Bažant, *Journal of Engineering Mechanics ASCE* 113 (1987) 379–390.
13. Y.R. Rashid, *Nuclear Engineering and Design* 7(4) (1968) 334–344.
14. J.G. Rots, *Ph.D. thesis*, TU-Delft, Delft (1988).
15. A. Saxena and S.J. Hudak Jr., *International Journal of Fracture* 14(5) (1978) 453–468.
16. J.E. Srawley, *International Journal of Fracture* 12 (1976) 475–476.
17. J.P.E. de Vree, W.A.M. Brekelmans and M.A.J. van Gils, *Computers & Structures* 55(4) (1995) 581–588.